Available online at www.sciencedirect.com
ScienceDirect
Acta Mathematica Scientia 2012,**32B**(1):129–154
Acta Mathematica Scientia 数学物理学报
http://actams.wipm.ac.cn

HOMOGENIZATION, SYMMETRY, AND PERIODIZATION IN DIFFUSIVE RANDOM MEDIA*

Dedicated to Professor Constantine M. Dafermos on the occasion of his 70th birthday

Alen Alexanderian
Department of Mechanical Engineering, Johns Hopkins University Baltimore, MD 21218, USA
E-mail: aalexa20@jhu.edu
Muruhan Rathinam† *Rouben Rostamian*‡
Department of Mathematics and Statistics, University of Maryland, Baltimore County
Baltimore, MD 21250, USA
E-mail: muruhan@umbc.edu; rostamian@umbc.edu

Abstract We present a systematic study of homogenization of diffusion in random media with emphasis on tile-based random microstructures. We give detailed examples of several such media starting from their physical descriptions, then construct the associated probability spaces and verify their ergodicity. After a discussion of material symmetries of random media, we derive criteria for the isotropy of the homogenized limits in tile-based structures. Furthermore, we study the periodization algorithm for the numerical approximation of the homogenized diffusion tensor and study the algorithm's rate of convergence. For one dimensional tile-based media, we prove a central limit result, giving a concrete rate of convergence for periodization. We also provide numerical evidence for a similar central limit behavior in the case of two dimensional tile-based structures.

Key words homogenization; periodization; random media; ergodic dynamical systems; material symmetry; isotropy

2000 MR Subject Classification 37A05; 37A25; 78M40; 35B27; 78A48

1 Introduction

In this article we present a general theory of homogenization of the steady-state diffusion equation in tile-based random media; these are defined as microstructures obtained by tiling the space with tiles of random diffusivities. There is a large body of literature on the homogenization of random media; cf. [5, 11, 19, 20, 24–26, 29, 36]. These generalize the more common study of the homogenization of periodic structures; see, e.g. [4, 12, 21, 23, 27].

*Received September 6, 2011.
†Research supported by the NSF grant DMS–0610013.
‡Corresponding author: Rouben Rostamian.

In Section 2 we state the homogenization theorem after setting up the basic tools and terminology. In Section 3 we study symmetry groups of random media and establish conditions that imply the isotropy of the homogenized limit.

The rest of the article specializes mostly to tile-based media which are introduced in Section 4. We set up the probability spaces from physical description of such media and show the ergodicity of the corresponding dynamical systems. Although ergodicity lies in the heart of the proof of convergence and homogenization, the practical verification of it is often cumbersome and therefore in the literature on random media it is common to assume, rather than verify ergodicity. In this article we make a point in verifying the ergodicity. In Section 5 we provide several examples of tile-based media to show the utility of the abstract theory and in Section 6 we further elaborate on these by examining their isotropy.

The characterization of the homogenized limit provided by the homogenization theorem, see Section 2, does not readily lend itself to numerical computations directly. Periodization provides a practical method for computing the homogenized diffusion tensor, the convergence of which was shown in [22] and [7]. For numerical studies via the method of periodization see [9] and [10]. Alternative numerical approaches are explored in [14, 15, 33].

In Section 7, after reviewing the general theory of periodization, we provide a self-contained convergence proof specialized to one-dimension. This helps to bring out the main idea of periodization in the general case, much in the same way that the proof of homogenization in one-dimensional media motivates the theory in higher dimensions. Specializing to one-dimensional tile-based media, we prove a Central Limit Theorem showing the rate of convergence of the sequence of periodized approximations of the diffusion coefficient. We supplement this with numerical results for illustration. Additionally, we provide computational results that demonstrate the convergence and a central limit behavior of the periodization in two-dimensions. We conclude with a conjecture on the rate of convergence. Such central limit behavior has been observed in numerical experiments reported in [34] in the context of heterogeneous multiscale methods. The reader may be interested in the article [35] that deals with a central limit type behavior for the rate of G-convergence of stochastic elliptic operators in dimension 3 or greater, and the articles [2, 17] that deal with the rate of convergence of discretized stochastic elliptic equations.

Central limit results for the convergence of solutions of boundary value problem to the homogenized limit may be found in [3, 6]. In contrast, our central limit results are concerned with the convergence of the periodized diffusion tensor to the homogenized tensor.

2 Preliminaries

In this section, we summarize notations and definitions that will be used throughout the remainder of this article.

2.1 Automorphisms

Following [13] we let:

Definition 1 An automorphism of a probability space $(\Omega, \mathcal{F}, \mu)$ is a bijection $\phi : \Omega \to \Omega$ such that for all $F \in \mathcal{F}$, $\phi(F)$ and $\phi^{-1}(F)$ belong to $\mathcal{F}$ and

$$\mu(F) = \mu\big(\phi(F)\big) = \mu\big(\phi^{-1}(F)\big).$$

We use the notation $\mathrm{Aut}(\Omega)$ to denote the set of all automorphisms on Ω.

2.2 Notation for matrices

We write $\mathbf{R}^{n\times n}$ for the space of $n \times n$ matrices. We let:

$\mathbf{R}^{n\times n}_{\mathrm{sym}}$ = the subspace of symmetric matrices in $\mathbf{R}^{n\times n}$,

$\mathbf{R}^{n\times n}_{\mathrm{orth}}$ = the orthogonal group of matrices in $\mathbf{R}^{n\times n}$,

$\mathbf{R}^{n\times n}_{\mathrm{orth}^+}$ = the proper orthogonal group of matrices in $\mathbf{R}^{n\times n}$.

For any $0 < \nu_1 \le \nu_2$ we let

$$E(\nu_1, \nu_2) = \{A \in \mathbf{R}^{n\times n}_{\mathrm{sym}} : \quad \nu_1|\xi|^2 \le \xi \cdot A\xi \le \nu_2|\xi|^2 \quad \forall \xi \in \mathbf{R}^n\}.$$

Let (S, Σ) be a measurable space. If $A : S \to \mathbf{R}^{n\times n}_{\mathrm{sym}}$ is a measurable mapping such that $A(x) \in E(\nu_1, \nu_2)$ for all $x \in S$ (or almost all $x \in S$ if there is a measure on (S, Σ)) then we say A belongs to $E(\nu_1, \nu_2, S)$.

2.3 The Dynamical System

An n-dimensional measure-preserving dynamical system T on Ω is a family of automorphisms $T_x : \Omega \to \Omega$, parametrized by $x \in \mathbf{R}^n$, satisfying:

1. $T_{x+y} = T_x \circ T_y$ for all $x, y \in \mathbf{R}^n$,
2. $T_0 = I$, where I is the identity map on Ω.
3. The dynamical system is jointly measurable on $\mathbf{R}^n \times \Omega$ in the sense that the mapping $(x, \omega) \mapsto T_x(\omega)$ is $\mathbb{B}(\mathbf{R}^n) \otimes \mathcal{F}/\mathcal{F}$ measurable, where $\mathbb{B}(\mathbf{R}^n)$ is the Borel σ-algebra on $\mathbf{R}^n$.

A set $E \subset \Omega$ is said to be invariant under the dynamical system T if $T_x^{-1}(E) \subset E$ for all $x \in \mathbf{R}^n$.

Definition 2 The dynamical system T is ergodic if all its invariant sets have measure of either zero or one.

The dynamical system T is ergodic if and only if for every measurable function $f : \Omega \to \mathbf{R}$ the following holds [13]:

$$\Big[f\big(T_x(\omega)\big) = f(\omega) \text{ for all } x \text{ and almost all } \omega \Big] \quad \Rightarrow \quad f = \text{constant a.s.} \tag{1}$$

Corresponding to a function $f : \Omega \to X$ (where X is any set) we define the function $f_T : \mathbf{R}^n \times \Omega \to X$ by

$$f_T\big(x, \omega\big) = f\big(T_x(\omega)\big), \quad x \in \mathbf{R}^n, \omega \in \Omega.$$

For each $\omega \in \Omega$, the function $f_T\big(\cdot, \omega\big) : \mathbf{R}^n \to X$ is called the realization of f for that ω.

2.4 Solenoidal and Potential Vector Fields

Let $(\Omega, \mathcal{F}, \mu)$ be a probability space with the σ-algebra $\mathcal{F}$ and a measure μ. We will write $E\{X\}$ for the expected value of the random variable X on Ω. That is, $E\{X\} = \int_\Omega X \,\mathrm{d}\mu$.

Let T be an n-dimensional measure-preserving dynamical system on Ω and let $L^2(\Omega; \mathbf{R}^n)$ be the space of square integrable vector fields $f : \Omega \to \mathbf{R}^n$. We define:

$$L^2_{\mathrm{pot}}(\Omega) = \{f \in L^2(\Omega; \mathbf{R}^n) : f_T(\cdot, \omega) \text{ is a potential field on } \mathbf{R}^n \text{ for almost all } \omega \in \Omega\},$$
$$L^2_{\mathrm{sol}}(\Omega) = \{f \in L^2(\Omega; \mathbf{R}^n) : f_T(\cdot, \omega) \text{ is a solenoidal field on } \mathbf{R}^n \text{ for almost all } \omega \in \Omega\},$$
$$\mathcal{V}^2_{\mathrm{pot}}(\Omega) = \big\{f \in L^2_{\mathrm{pot}}(\Omega) : E\{f\} = 0\big\}.$$
$$\mathcal{V}^2_{\mathrm{sol}}(\Omega) = \big\{f \in L^2_{\mathrm{sol}}(\Omega) : E\{f\} = 0\big\}.$$

These spaces induce orthogonal decompositions of $L^2(\Omega;\mathbf{R}^n)$, cf. [19, page 228]:

Theorem 1 (Weyl's Decomposition) If the dynamical system T is ergodic, then:

$$L^2(\Omega;\mathbf{R}^n) = \mathcal{V}^2_{\rm pot}(\Omega) \oplus L^2_{\rm sol}(\Omega) = \mathcal{V}^2_{\rm sol}(\Omega) \oplus L^2_{\rm pot}(\Omega). \tag{2}$$

2.5 Homogenization

Consider a matrix-valued function $A : \mathbf{R}^n \to \mathbf{R}^{n\times n}_{\rm sym}$. Assume that $A \in E(\nu_1,\nu_2,\mathbf{R}^n)$ for some $0 < \nu_1 \le \nu_2$.

For any $\epsilon > 0$ let $A^\epsilon(x) = A(x/\epsilon)$. Then we say that A admits homogenization if there exists a constant symmetric positive definite matrix A^0 such that for any bounded domain $\mathcal{D} \subset \mathbf{R}^n$ and any $f \in H^{-1}(\mathcal{D})$ the solutions u^ϵ and u^0 of the boundary value problems

$$\begin{cases} -\operatorname{div}(A^\epsilon \nabla u^\epsilon) = f & \text{on } \mathcal{D}, \\ u^\epsilon = 0 & \text{on } \partial\mathcal{D} \end{cases} \quad \text{and} \quad \begin{cases} -\operatorname{div}(A^0 \nabla u^0) = f & \text{on } \mathcal{D}, \\ u^0 = 0 & \text{on } \partial\mathcal{D} \end{cases} \tag{3}$$

satisfy, as $\epsilon \to 0$:

$$\begin{aligned} u^\epsilon &\rightharpoonup u^0 \quad &&\text{in} \quad H^1_0(\mathcal{D}), \\ A^\epsilon \nabla u^\epsilon &\rightharpoonup A^0 \nabla u^0 \quad &&\text{in} \quad L^2(\mathcal{D}). \end{aligned}$$

It is a classic result that if A is periodic on $\mathbf{R}^n$ then it admits homogenization. The basic references in [4, 12, 21, 23, 27] represent but a small sample of the vast literature on the subject.

The main focus of our article is on the random case, that is, the boundary value problem:

$$\begin{cases} -\operatorname{div}\Big(A\big(\frac{x}{\epsilon},\omega\big)\nabla u(x,\omega)\Big) = f(x) & \text{in } \mathcal{D}, \\ u(x,\omega) = 0 & \text{on } \partial\mathcal{D}, \end{cases} \tag{4}$$

where $\omega \in \Omega$ and $(\Omega, \mathcal{F}, \mu)$ is a probability space.

A fully developed theory exists for the case when $A : \mathbf{R}^n \times \Omega \to \mathbf{R}^{n\times n}_{\rm sym}$ is a stationary and ergodic random field. The early work in the area [20, 24] is greatly expanded upon in the monograph [19]. In this theory, without loss of generality, one begins with a function $\mathcal{A} \in E(\nu_1,\nu_2,\Omega)$ and considers its realizations $A(x,\omega) = \mathcal{A}_T(x,\omega)$ with respect to an n-dimensional ergodic dynamical system T. Concerning this, we have:

Theorem 2 [19, Theorem 7.4] Let $\mathcal{A} \in E(\nu_1,\nu_2,\Omega)$ and T be an n-dimensional measure-preserving ergodic dynamical system on Ω. Then, for almost all $\omega \in \Omega$, the realization $\mathcal{A}_T(\cdot,\omega)$ admits a homogenization $\mathcal{A}^0$. Moreover, $\mathcal{A}^0$ is positive-definite, independent of ω, and is characterized by,

$$\xi \cdot \mathcal{A}^0 \xi = \inf_{v \in \mathcal{V}^2_{\rm pot}(\Omega)} \int_\Omega (\xi + v)\cdot \mathcal{A}(\xi + v)\mathrm{d}\mu, \quad \forall \xi \in \mathbf{R}^n. \tag{5}$$

Remark 1 Although Theorem 2 gives a complete characterization of the limiting homogenized problem, the characterization is not constructive because it involves integrating on an abstract probability space. The method of periodization [7, 22], described in Section 7, provides a concrete way of approximating $\mathcal{A}^0$ numerically.

2.6 Linear Algebra

Here we collect some observations and results from linear algebra, which will be needed in our discussions of symmetry and isotropy.

A subspace $V \subseteq \mathbf{R}^n$ is said to be invariant under $A \in \mathbf{R}^{n\times n}$ if $AV \subseteq V$.

Definition 3 (Irreducible group [31]) Let G be a matrix group in $\mathbf{R}^{n\times n}$. We call G an irreducible group if it has the following property: If a subspace V of $\mathbf{R}^n$ is invariant under Q for all $Q \in G$, then V is either $\{0\}$ or $\mathbf{R}^n$.

As an example of an irreducible group in $\mathbf{R}^{2\times 2}$ consider the cyclic rotation group of order 4: $G_1 = \{I, R_{90}, R_{180}, R_{270}\}$, where $R_\theta \in \mathbf{R}^{2\times 2}$ denotes rotation by angle θ about the origin. Another example of an irreducible group is $\mathbf{R}^{n\times n}_{\text{orth}^+}$. An example of a group which is not irreducible is $G_2 = \{I, R_{180}\}$ because it leaves any one-dimensional subspace invariant.

The following result is a simple case of Schur's Lemma [28], (also [16, 18]) which is a basic result in group representation theory.

Lemma 1 Let G be an irreducible group in $\mathbf{R}^{n\times n}$ and suppose A is a symmetric matrix that commutes with every $Q \in G$. Then A is a scalar multiple of identity.

Proof Let α be an eigenvalue of A, and define the mapping $B = A - \alpha I$. It follows that, $BQ = QB$ for all $Q \in G$. Moreover, since α is an eigenvalue of A, $\text{Null}(B) = \text{Null}(A-\alpha I) \neq \{0\}$. Now, if $x \in \text{Null}(B)$, then $BQx = QBx = 0$, that is $Qx \in \text{Null}(B)$. Therefore, $\text{Null}(B)$ is invariant under Q for all $Q \in G$. Since G is irreducible (and $\text{Null}(B) \neq \{0\}$), it follows that $\text{Null}(B) = \mathbf{R}^n$. That is, $B = 0$, and hence $A = \alpha I$. □

Let us give an example that shows that the condition of irreducibility in Lemma 1 cannot be removed. Consider the symmetric 2×2 matrix $A = \begin{pmatrix} a & b \\ b & c \end{pmatrix}$. Suppose A commutes with elements of the reducible group $G = \{I, R\}$ where $R = \begin{pmatrix} 1 & 0 \\ 0 & -1 \end{pmatrix}$. Then $AR = RA$ implies that $b = 0$ whence $A = \begin{pmatrix} a & 0 \\ 0 & c \end{pmatrix}$ where a and c are arbitrary.

The following two results give conditions under which a matrix is a multiple of identity in two and three dimensions.

Proposition 1 Let $S \in \mathbf{R}^{2\times 2}_{\text{sym}}$ and $Q \in \mathbf{R}^{2\times 2}_{\text{orth}^+} \setminus \{\pm I\}$. Then S commutes with Q if and only if $S = \lambda I$.

Proof Suppose $SQ = QS$. The only subspace of $\mathbf{R}^2$ invariant under Q is either $\{0\}$ or $\mathbf{R}^2$. Hence, the result follows from Lemma 1. The converse implication is trivial. □

Proposition 2 Let u and v be linearly independent vectors in $\mathbf{R}^3$. Fix α and β in $(0, \pi)$. Suppose $S \in \mathbf{R}^{3\times 3}_{\text{sym}}$ commutes with R^α_u and R^β_v. Then S is a multiple of identity.

Proof We will show that the only subspaces of $\mathbf{R}^3$ invariant under both R^α_u and R^β_v are $\{0\}$ and $\mathbf{R}^3$; the result would then follow from Lemma 1. Note that the only subspaces of $\mathbf{R}^3$ invariant under R^α_u are:

$$\{0\}, \quad \text{span}\{u\}, \quad \text{span}\{u\}^\perp, \quad \mathbf{R}^3.$$

Similarly, the only subspaces of $\mathbf{R}^3$ invariant under R^β_v are:

$$\{0\}, \quad \text{span}\{v\}, \quad \text{span}\{v\}^\perp, \quad \mathbf{R}^3.$$

Since u and v are linearly independent, it follows that $\{0\}$ and $\mathbf{R}^3$ are the only subspaces of $\mathbf{R}^3$ invariant under both R^α_u and R^β_v. □

3 Symmetries of Random Media and Questions of Isotropy

In this section we develop an abstract framework and study interesting but nontrivial conditions on the conductivity matrix $\mathcal{A}_T(x,\omega)$ which imply that the homogenized conductivity matrix, $\mathcal{A}^0$, is a multiple of identity, that is, the homogenized medium is isotropic.

Definition 4 Let Q be an orthogonal matrix and T be a dynamical system. We say that $\mathcal{A} \in E(\nu_1,\nu_2,\Omega)$ is Q-invariant if there exists $\zeta \in \mathrm{Aut}(\Omega)$ such that:

$$\mathcal{A}_T\big(x,\zeta(\omega)\big) = Q\mathcal{A}_T(Q^T x,\omega)Q^T,$$

for almost all $x \in \mathbf{R}^n$ and almost all $\omega \in \Omega$.

Remark 2 The above definition can be best understood in terms of the commutative diagram in Figure 1. Let $\mathcal{M} = E(\nu_1,\nu_2,\mathbf{R}^n)$, and let $i : \Omega \to \mathcal{M} : \omega \mapsto \mathcal{A}_T(\cdot,\omega)$; that is, $i(\omega)$ is the conductivity tensor field corresponding to $\omega \in \Omega$. Given $Q \in \mathbf{R}^{n\times n}_{\mathrm{orth}}$, we define $\mathbb{Q} : \mathcal{M} \to \mathcal{M}$ by

$$(\mathbb{Q}\mathcal{A}_T)(x,\omega) = Q\mathcal{A}_T(Q^T x,\omega)Q^T.$$

From Definition 4, it follows that the diagram in Figure 1 commutes. This means that any collection $M \subset \mathcal{M}$ of conductivity tensors and their rotated versions $\mathbb{Q}M$ are equally likely, that is, $\mu\big(i^{-1}(M)\big) = \mu\big(i^{-1}(\mathbb{Q}M)\big)$. This follows since,

$$\mu\big(i^{-1}(\mathbb{Q}M)\big) = \mu\big(\zeta^{-1}i^{-1}(\mathbb{Q}M)\big) = \mu\big(i^{-1}\mathbb{Q}^{-1}\mathbb{Q}(M)\big) = \mu\big(i^{-1}(M)\big),$$

where the first equality holds since ζ is measure preserving, and the second equality holds since the diagram in Figure 1 commutes.

$$\begin{tikzcd}
\Omega \arrow[r, "i"] \arrow[d, "\zeta"'] & \mathcal{M} \arrow[d, "\mathbb{Q}"] \\
\Omega \arrow[r, "i"] & \mathcal{M}
\end{tikzcd}$$

Fig.1 Diagram showing invariance under Q

Proposition 3 Suppose $\mathcal{A}$ is Q-invariant for a given $Q \in \mathbf{R}^{n\times n}_{\mathrm{orth}^+}$. Then the corresponding homogenized matrix $\mathcal{A}^0$ commutes with Q, that is, $\mathcal{A}^0 Q = Q\mathcal{A}^0$.

Proof We know by Theorem 2 that $\mathcal{A}_T(x,\omega)$ admits homogenization $\mathcal{A}^0$ almost surely. Moreover, by Q-invariance

$$\mathcal{A}_T\big(x,\zeta(\omega)\big) = Q\mathcal{A}_T(Q^T x,\omega)Q^T, \tag{6}$$

where $\zeta \in \mathrm{Aut}(\Omega)$. Since ζ is measure preserving, $\mathcal{A}_T\big(x,\zeta(\omega)\big)$ admits homogenization $\mathcal{A}^0$ almost surely, and using (6), $Q\mathcal{A}_T(Q^T x,\omega)Q^T$ admits homogenization $\mathcal{A}^0$ also. On the other hand, it is straightforward to see that $\mathcal{B}(x,\omega) = Q\mathcal{A}_T(Q^T x,\omega)Q^T$ admits homogenization $Q\mathcal{A}^0Q^T$ for almost all $\omega \in \Omega$ (this follows by performing a change of coordinates in the definition of homogenization). Therefore, $\mathcal{A}^0 = Q\mathcal{A}^0Q^T$, and hence the result. $\square$

Theorem 3 Suppose $\mathcal{A}$ is Q-invariant for all $Q \in G$, where G is an irreducible group. Then, the corresponding homogenized matrix $\mathcal{A}^0$ is isotropic, that is, $\mathcal{A}^0 = \lambda I$ where λ is a constant scalar.

Proof By Proposition 3, we know that $\mathcal{A}^0$ commutes with all $Q \in G$. The result follows from Lemma 1. □

Remark 3 The proof of the analogous result for the system of equations of linear elastostatics is substantially more involved. For a comprehensive study of the questions of isotropy of linearly elastic materials see [1].

3.1 Special Cases of 2D and 3D

Here we give sufficient conditions for isotropy of the homogenized matrix $\mathcal{A}^0$ in two and three dimensions. The case of two dimensions is addressed by the following proposition.

Proposition 4 Suppose $\mathcal{A}$ is Q-invariant for a given $Q \in \mathbf{R}^{2\times 2}_{\text{orth}^+} \setminus \{\pm I\}$. Then, the corresponding homogenized matrix $\mathcal{A}^0$ is isotropic; that is $\mathcal{A}^0 = \lambda I$ where λ is a constant.

Proof The result follows from Proposition 3 and Proposition 1. □

In the case of $\mathbf{R}^3$ we can appeal to our linear algebra developments above.

Proposition 5 Suppose $\mathcal{A}$ is both R_u^α-invariant and R_v^β-invariant, where R_u^α and R_v^β are as in Proposition 2. Then, the corresponding homogenized matrix $\mathcal{A}^0$ is isotropic, that is, $\mathcal{A}^0 = \lambda I$ where λ is a constant.

Proof The result follows from Proposition 3 and Proposition 2. □

4 Tile-based Random Media: General Theory

The general theory of random media described in the previous sections is based on characterization of a random medium in terms of an abstract probability space and a dynamical system acting on it. The physical properties of such a medium are then obtained through the realization formalism described in Section 2.3.

The more interesting problem, in practice, is the reverse; that is, to construct the probability space and a dynamical system, starting from the the physical description of the random medium. Although this process is an essential aspect of the modeling of random media, it is rarely brought out and analyzed in detail in the literature. It is among our goals in this article to bring this issue to focus. As we will see in the following sections, the process is not quite trivial.

In Section 4.1 we introduce the set Y of all possible tiles, and put a probability measure on it. In the simplest case of a "black-white" checkerboard where the tiles can be only one of two possibilities, the set Y consists of two elements and the probability measure indicates the likelihood of occurrence of one or the other tile. Subsequently, we use Y as building blocks for the sample space of all possible realizations. In Section 4.2 we construct a dynamical system $\{T_x\}_{x\in\mathbf{R}^n}$ on the probability space which tiles the space with random tiles from the set Y. We show that the dynamical system is measure preserving and ergodic. In Section 4.3 we start with the physical description of the conductivity tensor $A^{(y)}$ of each tile y in Y and construct the overall conductivity tensor $A_T(x,\omega)$ that enters the boundary value problem (3). The constructions are rather abstract but they are sufficiently general to include many interesting applications as illustrated in Section 5.

4.1 The Probability Space

Let the set Y parametrize the possible choices for a tile and consider the probability space $(Y, \mathcal{F}_Y, \mu_Y)$, where $\mathcal{F}_Y$ is an appropriate σ-algebra and μ_Y is a probability measure. Form the product space $(S, \mathcal{F}_S, \mu_S) = \prod_{\mathbf{Z}^n}(Y, \mathcal{F}_Y, \mu_Y)$, where the σ-algebra $\mathcal{F}_S$ is the product σ-algebra and μ_S is the product measure. Finally, to account for translations, define the overall probability space

$$(\Omega, \mathcal{F}, \mu) = (S, \mathcal{F}_S, \mu_S) \otimes \big(\mathbf{Tor}^n, \mathbb{B}(\mathbf{Tor}^n), \mathrm{Leb}\,\big), \tag{7}$$

where $\mathbf{Tor}^n = [0,1)^n$ is the n-dimensional unit cube with the opposite faces identified, $\mathbb{B}(\mathbf{Tor}^n)$ is the Borel σ-algebra on $\mathbf{Tor}^n$, and Leb is the Lebesgue measure.

4.2 The Dynamical System and Ergodicity

We construct the measure-preserving and ergodic dynamical system T that enters the definition of the conductivity matrix in the boundary value problem (4). An element $s \in S$ has form

$$s = \{s_j\}_{j \in \mathbf{Z}^n}, \quad s_j \in Y,$$

and an element $\omega \in \Omega$ has form,

$$\omega = (s, \tau) \quad s \in S,\, \tau \in \mathbf{Tor}^n. \tag{8}$$

First we define the dynamical system $\{\hat{T}_z\}_{z \in \mathbf{Z}^n}$ on S by

$$\hat{T}_z\big(\{s_j\}_{j \in \mathbf{Z}^n}\big) = \{s_{j+z}\}_{j \in \mathbf{Z}^n}.$$

Let us define the projection operators $P_1 : \mathbf{R}^n \to \mathbf{Z}^n$ and $P_2 : \mathbf{R}^n \to \mathbf{Tor}^n$ by

$$\begin{aligned} P_1(x) &= \lfloor x \rfloor, \quad x \in \mathbf{R}^n, \\ P_2(x) &= x - \lfloor x \rfloor, \quad x \in \mathbf{R}^n. \end{aligned}$$

Here $\lfloor x \rfloor$ is the vector whose elements are the greatest integers less or equal to the corresponding elements in x. Note that each $x \in \mathbf{R}^n$ has the unique decomposition

$$x = P_1(x) + P_2(x).$$

Next, define the dynamical system $\{\hat{R}_x\}_{x \in \mathbf{R}^n}$ on $\mathbf{Tor}^n$ by

$$\hat{R}_x(\tau) = P_2(x + \tau), \quad \tau \in \mathbf{Tor}^n.$$

Finally, we define the dynamical system $\{T_x\}_{x \in \mathbf{R}^n}$ on Ω by

$$T_x(\omega) = T_x(s, \tau) = \big(\hat{T}_{P_1(x+\tau)}(s),\, \hat{R}_x(\tau)\big), \quad s \in S,\, \tau \in \mathbf{Tor}^n. \tag{9}$$

Let us verify the group property for the dynamical system above. Clearly $T_0(\omega) = \omega$ for all $\omega \in \Omega$. Moreover, we show $T_x \circ T_y = T_{x+y}$ for all x and y in $\mathbf{R}^n$ as follows. Let $\omega = (s, \tau)$ be an element of Ω, as described in (8), and note that

$$T_{x+y}(\omega) = T_{x+y}(\{s_j\}, \tau) = \big(\{s_{j+P_1(x+y+\tau)}\}, P_2(x + y + \tau)\big)\,. \tag{10}$$

On the other hand

$$\begin{aligned} T_x\big(T_y(\omega)\big) &= T_x\Big(T_y\big(\{s_j\},\tau\big)\Big) = T_x\Big(\{s_{j+P_1(y+\tau)}\}, P_2(y+\tau)\Big) \\ &= \Big(\{s_{j+P_1(y+\tau)+P_1(x+P_2(y+\tau))}\}, P_2\big(x+P_2(y+\tau)\big)\Big). \end{aligned} \tag{11}$$

Since $u + P_1(v) = P_1(u+v)$ for every $u \in \mathbf{Z}^n, v \in \mathbf{R}^n$, we have

$$P_1(y+\tau) + P_1\big(x+P_2(y+\tau)\big) = P_1\big(x+P_1(y+\tau)+P_2(y+\tau)\big) = P_1(x+y+\tau). \tag{12}$$

Also, since $P_2(u+v) = P_2(v)$ for every $u \in \mathbf{Z}^n$ and $v \in \mathbf{R}^n$, we have,

$$P_2\big(x+P_2(y+\tau)\big) = P_2\big(x+P_1(y+\tau)+P_2(y+\tau)\big) = P_2(x+y+\tau). \tag{13}$$

Combining (11), (12), and (13) we obtain

$$T_x\big(T_y(\omega)\big) = \big(\{s_{j+P_1(x+y+\tau)}\}, P_2(x+y+\tau)\big) = T_{x+y}(\omega),$$

where the last equality follows from (10).

The measure preserving property of the dynamical system $\{T_x\}_{x\in\mathbf{R}^n}$ follows from the following proposition:

Proposition 6 The dynamical system $\{T_x\}_{x\in\mathbf{R}^n}$ defined in (9) is measure preserving.

Proof Let $x \in \mathbf{R}^n$ be fixed but arbitrary. It is sufficient so show that $\mu\big(T_x^{-1}(A\times B)\big) = \mu(A\times B)$ for all rectangles $A\times B \in \mathcal{F}$, where $A \in \mathcal{F}_S$ and $B \in \mathbb{B}(\mathbf{Tor}^n)$. Note that we can partition $\mathbf{Tor}^n$ as follows,

$$\mathbf{Tor}^n = \biguplus_{j\in\mathbf{Z}^n} E_j, \quad E_j = \{\tau \in \mathbf{Tor}^n : P_1(x+\tau) = j\},$$

where $\biguplus$ denotes a disjoint union. Note also that only finitely many of E_j are non-empty. Then, for a rectangle $A\times B$ in $\mathcal{F}$ we have

$$T_x^{-1}(A\times B) = \biguplus_j \Big(\hat{T}_j^{-1}(A) \times \big[\hat{R}_x^{-1}(B)\cap E_j\big]\Big).$$

Since $\hat{T}_j$ and $\hat{R}_x$ are measure preserving, we conclude that

$$\begin{aligned} \mu\big(T_x^{-1}(A\times B)\big) &= \sum_j \mu\Big(\hat{T}_j^{-1}(A)\times\big[\hat{R}_x^{-1}(B)\cap E_j\big]\Big) = \sum_j \mu_S(A)\,\mathrm{Leb}[\hat{R}_x^{-1}(B)\cap E_j] \\ &= \mu_S(A)\sum_j \mathrm{Leb}\left[\hat{R}_x^{-1}(B)\cap E_j\right] = \mu_S(A)\,\mathrm{Leb}\left(\hat{R}_x^{-1}(B)\right) \\ &= \mu_S(A)\,\mathrm{Leb}(B) = \mu(A\times B). \end{aligned} \tag{14}$$

□

What remains to show is ergodicity of the dynamical system T_x. It is well-known that the dynamical system $\{\hat{T}_z\}_{z\in\mathbf{Z}^n}$ is ergodic [13, 30]. We use this to prove the following:

Proposition 7 The dynamical system $\{T_x\}_{x\in\mathbf{R}^n}$ defined in (9) is ergodic.

Proof Let f be a measurable function on Ω which is invariant under T, that is,

$$f\big(T_x(\omega)\big) = f(\omega) \quad \forall x \in \mathbf{R}^n,\ \mu\text{-a.s.}. \tag{15}$$

Recall that $\omega \in \Omega$ has the form $\omega = (s, \tau)$, with $s \in S$ and $\tau \in \mathbf{Tor}^n$. Now by (15) we have also $f\big(T_z(\omega)\big) = f(\omega)$, for all $z \in \mathbf{Z}^n$. Since $\hat{R}_z(\tau) = \tau$ for $z \in \mathbf{Z}^n$,

$$f(s,\tau) = f\big(T_z(s,\tau)\big) = f\big(\hat{T}_z(s), \hat{R}_z(\tau)\big) = f\big(\hat{T}_z(s), \tau\big).$$

Letting $f^\tau(s) = f(s,\tau)$, this takes the form

$$f^\tau\big(\hat{T}_z(s)\big) = f^\tau(s) \quad \forall z \in \mathbf{Z}^n. \tag{16}$$

We know $f^\tau(s)$ is measurable on S. Since $\{\hat{T}_z\}_{z\in\mathbf{Z}^n}$ is ergodic, then (16) implies that for each τ, f^τ is constant μ_S-a.s.. Therefore,

$$f(s,\tau) = \phi(\tau) \quad s \in S,\ \tau \in \mathbf{Tor}^n. \tag{17}$$

Next, using (15) again we have

$$f\big(T_t(\omega)\big) = f(\omega) \quad \forall t \in \mathbf{Tor}^n. \tag{18}$$

Now, using (17) we have

$$f\big(T_t(\omega)\big) = f\big(\hat{T}_{P_1(t+\tau)}(s), \hat{R}_t(\tau)\big) = \phi(\hat{R}_t\tau);$$

also, $f(\omega) = f(s,\tau) = \phi(\tau)$. Therefore, (18) gives that

$$\phi\big(\hat{R}_t(\tau)\big) = \phi(\tau) \quad \forall t \in \mathbf{Tor}^n, \text{ a.e.} \tag{19}$$

Finally, recalling ergodicity of the dynamical system $\{\hat{R}_t\}_{t\in\mathbf{Tor}^n}$, we get that $\phi(\tau) \equiv$ const a.e. and hence, $f \equiv$ const a.e. Thus, the assertion of the proposition follows from (1). $\square$

4.3 The Function $\mathcal{A}$

Each element y in the sample space Y specifies a certain type of tile. Let $A^{(y)} : \mathbf{Tor}^n \to \mathbf{R}^{n\times n}_{\text{sym}}$ be the conductivity function associated with that tile. Pick $s \in S$ and let's write $s = \{s_j\}_{j\in\mathbf{Z}^n}$. This defines an infinite sequence of tiles with conductivities $\{A^{(s_j)}\}_{j\in\mathbf{Z}^n}$. We define the random variable $\mathcal{A} : \Omega \to \mathbf{R}^{n\times n}_{\text{sym}}$ by

$$\mathcal{A}(\omega) = A^{(s_0)}(\tau), \quad \text{for } \omega = \big(\{s_j\}, \tau\big) \in \Omega. \tag{20}$$

From the definition T_x in (9) we see that:

$$T_x(\omega) = T_x\big(\{s_j\}, \tau\big) = \big(\{s_{j+P_1(x+\tau)}\}, P_2(x+\tau)\big).$$

Consequently,

$$\mathcal{A}\big(T_x(\omega)\big) = A^{(s_\sigma)}\big(P_2(x+\tau)\big), \quad \text{where } \sigma = P_1(x+\tau).$$

Let us recall that $A_T(x,\omega) = \mathcal{A}\big(T_x(\omega)\big)$ defines the conductivity matrix of the medium and appears as a coefficient in the boundary value problem (4).

5 Tile-based Random Media: Examples

In the following sections we give several examples to illustrate the construction of concrete probability spaces in terms of the medium's physical properties. In each case, it suffices to identify the probability space $(Y, \mathcal{F}_Y, \mu_Y)$ and the tile conductivities $A^{(y)}$ as defined in Section 4.3. The machinery developed in Section 4 then assigns the appropriate dynamical system and the conductivity tensor $\mathcal{A}$.

5.1 Checkerboard-like Tilings

For our first example we examine a most basic random structure—an n-dimensional medium consisting of the n-dimensional cube $(0,1)^n$ and its translations along the integer lattice $\mathbf{Z}^n$ in $\mathbf{R}^n$. The cubes/tiles are identified as either gray or white with probabilities p and $1-p$, respectively, where $p \in (0,1)$. Figure 2 depicts representative samples in 1, 2, and 3 dimensions.

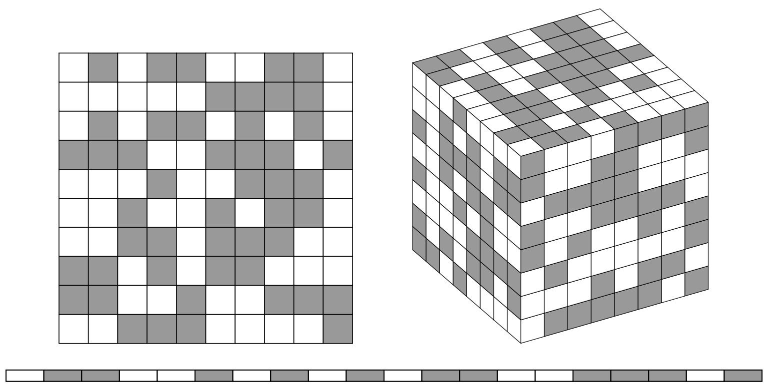

Fig.2 Typical realizations of random "checkerboards" in one, two, or three dimensions

Define the space Y of Section 4.1 as the set $Y = \{\text{gray}, \text{white}\}$. On the measurable space $(Y, 2^Y)$ define the measure μ_Y as

$$\mu_Y\big(\{\text{gray}\}\big) = p, \quad \mu_Y\big(\{\text{white}\}\big) = 1 - p.$$

The squares (or cubes) are characterized by their conductivity matrices $A^{(\text{gray})}$ and $A^{(\text{white})}$, each of which is a function $\mathbf{Tor}^n \to \mathbf{R}^{n\times n}_{\text{sym}}$. In particular, if the tiles are made of homogeneous materials, then these conductivities are constant functions.

5.2 Randomly Rotated Ellipses

Consider a two-dimensional, two-phase structure consisting of randomly rotated homogeneous congruent elliptic grains embedded within homogeneous square tiles. We assume that the ellipses are centered at the centers of the tiles and are sufficiently small so that they do not extend beyond tile boundaries. We tile the two-dimensional plane with these, as in Figure 3.

The construction of the probability space for this structure amounts to specifying the state space $(Y, \mathcal{F}_Y, \mu_Y)$, the rest of the construction remains as before. We let $Y = [0, \pi)$ represent the set of rotation angles and we set $F_Y = \mathbb{B}(Y)$ and $\mu_Y(E) = \frac{1}{\pi}\,\text{Leb}(E)$, for all $E \in \mathcal{F}_Y$, implying that the rotation angles are uniformly distributed on $[0, \pi)$.

The conductivity matrix $A^{(\theta)} : \mathbf{Tor}^2 \to \mathbf{R}^{2\times 2}_{\mathrm{sym}}$ for each rotation angle $\theta \in Y$ is defined as

$$A^{(\theta)}(x) = \begin{cases} \alpha_1 I & \text{if } x \in \mathcal{E}_\theta, \\ \alpha_2 I & \text{if } x \notin \mathcal{E}_\theta, \end{cases}$$

where α_1 and α_2 are positive constants and $\mathcal{E}_\theta$ is the interior of the rotated ellipse.

5.3 Variable-size Circular Grains

Consider a two-dimensional, two-phase structure consisting of homogeneous circular grains of varying sizes embedded within homogeneous square tiles. We assume that the circles are centered at the centers of the tiles and are sufficiently small so that the do not extend beyond tile boundaries. We tile the two-dimensional plane with these, as in Figure 4. The circle radii are distributed randomly in the interval $[r_0, r_1]$. Thus we have $Y = [r_0, r_1]$, $F_Y = \mathbb{B}(Y)$ and $\mu_Y(E) = \frac{1}{r_1 - r_0}\,\mathrm{Leb}(E)$ for all $E \in \mathcal{F}_Y$.

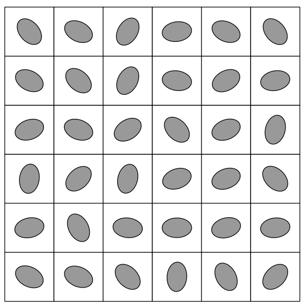

Fig.3 A tile-based medium tiled with randomly rotated ellipses

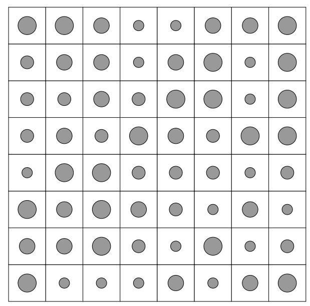

Fig.4 A tile-based medium tiled with randomly sized and perturbed circles

The conductivity matrix $A^{(r)} : \mathbf{Tor}^2 \to \mathbf{R}^{2\times 2}_{\mathrm{sym}}$ for each $r \in Y$ is defined as

$$A^{(r)}(x) = \begin{cases} \alpha_1 I & \text{if } x \in \mathcal{C}_r, \\ \alpha_2 I & \text{if } x \notin \mathcal{C}_r, \end{cases}$$

where α_1 and α_2 are positive constants and $\mathcal{C}_r$ is the interior of the circle of radius r.

This example may be modified easily to allow random perturbations of the circle centers relative to the tile. Suppose the centers are disturbed by the amounts δ_x and δ_y in the x and y directions, where δ_x and δ_y are distributed uniformly in the intervals $[-\alpha, +\alpha]$ and $[-\beta, +\beta]$, respectively. Also assume that r_0, r_1, α and β are such that the circles don't overlap; see Figure 5. In this case, we have $Y = [-\alpha, +\alpha] \times [-\beta, +\beta] \times [r_0, r_1]$, $\mathcal{F}_Y = \mathbb{B}(Y)$, and $\mu_Y(E) = \mathrm{Leb}(E)/\big(4\alpha\beta(r_1 - r_0)\big)$ for all $E \in \mathcal{F}_Y$. The conductivity matrix may be defined much in the same way as before.

5.4 Random Honeycomb

Here we construct a two-dimensional two-phase random honeycomb structure. The constructions and the arguments are similar to the case of structures based on rectangular lattice presented in the previous subsection.

Consider a honeycomb structure as depicted in Figure 6, consisting of a regular hexagonal tiling of the plane, where each hexagon has side-length one and is made of a homogeneous material chosen randomly from among two possibilities of either gray or white with probabilities

p and $1-p$. The construction of the probability space, the dynamical system, and the function $\mathcal{A}$ is similar to the random checkerboard except for the following two differences: 1) In the construction of the probability space, we replace $\mathbf{Tor}^2$ with H, where H is the hexagon of unit side-length centered at the origin with its opposite sides identified. 2) In the construction of the dynamical system T, we redefine the projections P_1 and P_2. Each hexagon is identified by the integer pair (m,n) that defines the hexagon's position through $c = mv_1 + nv_2$ where $\{v_1, v_2\}$ is a lattice basis. For example we may let, $\mathbf{v_1} = \langle\sqrt{3}, 0\rangle$, $\mathbf{v_2} = \langle\sqrt{3}/2, 3/2\rangle$. Then, given any $x \in \mathbf{R}^2$, there is a unique $h \in H$ and $(m_1, m_2) \in \mathbf{Z}^2$ such that $x = h + [m_1\mathbf{v_1} + m_2\mathbf{v_2}]$. Accordingly, we define $P_1(x) = \langle m_1, m_2\rangle$ and $P_2(x) = h$. The construction of a stationary and ergodic dynamical system proceeds in the same way as in the case of the checkerboard-like structures.

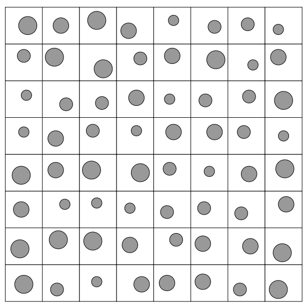

Fig.5 A tile-based medium tiled with randomly sized circles

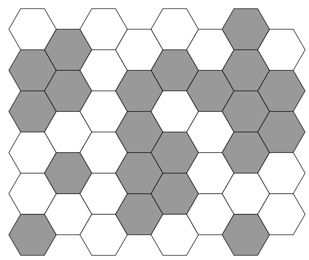

Fig.6 A random honeycomb structure

6 Tile-based Random Media: Isotropy

In this section, we apply the isotropy results of Section 3 to several concrete examples.

6.1 Random Checkerboard

Recall the two-dimensional random checkerboard constructed in Section 5.1. Let us assume the conductivity matrices $A^{(\text{gray})}$ and $A^{(\text{white})}$ are isotropic, that is $A^{(\text{gray})} = a_1 I$ and $A^{(\text{white})} = a_2 I$, where a_1 and a_2 are positive constants and I is the identity matrix. The following result, which is not new—see [19, page 237] for example—is a consequence of our Proposition 4.

Proposition 8 The homogenized material corresponding to the checkerboard constructed as above is isotropic, that is, $\mathcal{A}^0$ is a multiple of identity.

Proof Let Q be a 90 degree rotation of the plane. Consider the realization $\mathcal{A}\big(T_{Q^Tx}(\omega)\big)$. This corresponds to another realization, say $\mathcal{A}\big(T_x(\omega')\big)$, for some $\omega' \in \Omega$. We let $\zeta(\omega) = \omega'$. Note that $\zeta : \Omega \to \Omega$ sends the element $\omega = \big(\{s_j\}, \tau\big) \in \Omega$ to $\omega' = \big(\{s_{\sigma(j)}\}, \rho(\tau)\big) \in \Omega$, where $\big\{\sigma(j)\big\}_{j\in\mathbf{Z}^2}$ is a permutation of $\big\{j\big\}_{j\in\mathbf{Z}^2}$ and ρ is an affine map involving rotations and translations on $\mathbf{Tor}^2$. Both of these are measure preserving maps, therefore ζ is measure preserving; thus $\mathcal{A}$ is Q-invariant and the assertion follows from Proposition 4. □

Remark 4 Proposition 8 remains true if the coefficients a_1 and a_2 are variable as long as they are invariant under 90 degree rotations of $\mathbf{Tor}^2$.

6.2 Three-dimensional Random "Checkerboard"

Recall the three-dimensional random checkerboard constructed in Section 5.1. Let us assume the conductivity matrices $A^{(\mathrm{gray})}$ and $A^{(\mathrm{white})}$ are multiples of identity, that is $A^{(\mathrm{gray})} = a_1 I$ and $A^{(\mathrm{white})} = a_2 I$, where a_1 and a_2 are positive constants.

Proposition 9 The homogenized material corresponding to the three-dimensional checkerboard constructed as above is isotropic, that is, $\mathcal{A}^0$ is a multiple of identity.

Proof Let R_x^{90} and R_y^{90} be 90 degree rotations about the x and y axes. The result follows by noting that $\mathcal{A}$ is R_x^{90}-invariant and R_y^{90}-invariant and applying Proposition 5. □

6.3 Random Honeycomb

Consider the random honeycomb constructed in Section 5.4. Let us assume the conductivity matrices $A^{(\mathrm{gray})}$ and $A^{(\mathrm{white})}$ are multiples of identity, that is $A^{(\mathrm{gray})} = a_1 I$ and $A^{(\mathrm{white})} = a_2 I$, where a_1 and a_2 are positive constants.

Proposition 10 The homogenized material corresponding to the random honeycomb constructed as above is isotropic, that is, $\mathcal{A}^0$ is a multiple of identity.

Proof Let Q be the 2×2 matrix of rotation by $\pi/3$. The result follows by noting that $\mathcal{A}$ is Q-invariant and applying Proposition 4. □

7 Numerical Computations and Periodization

The homogenized limit $\mathcal{A}^0$ of a random medium, characterized by formula (5) in Theorem 2, involves integration on the abstract probability space Ω. This is not practical for explicit computations. The method of periodization, introduced in [22], is a practical approximation scheme for computing homogenized limits of random media. Also see [7] for further work along these lines and [9, 10] for numerical experiments.

Periodization proceeds by fixing a single realization $\omega \in \Omega$ of the random structure. Then one cuts a cube $S_\rho = [0, \rho]^n$ of size ρ from it, then tiles the space periodically with that cube. Then the homogenized limit $\mathcal{A}^\rho(\omega)$ of the resulting periodic medium is computed in the usual way; e.g., [4, 27]. It is shown in [22] and [7] that

$$\mathcal{A}^\rho(\omega) \to \mathcal{A}^0 \text{ almost surely, as } \rho \to \infty, \tag{21}$$

where $\mathcal{A}^0$, given by formula (5), is independent of ω.

The purpose of this section is to place the method of periodization in the context of the theory of tile-based media that we have developed in the previous sections. In Subsection 7.1 we analyze the periodization process in one-dimensional tile-based media. These computations are quite explicit since the partial differential equation of equilibrium reduces to an ordinary differential equation. Although the one-dimensional results are straightforward to derive, there is no convenient place in the literature for reference, therefore we have seen it appropriate to gather these results here.

Theorem 4 gives a self-contained proof of the periodization theorem in 1D, via Birkhoff's Ergodic Theorem. Theorem 5 establishes a central limit result which provides the rate of convergence of the diffusion coefficient with successive improvements of the periodization approximation. In Subsection 7.2.2 we give results of a series of numerical experiments whose purpose is to illustrate the theory developed up to that point.

Section 7.3 reports the results of numerical experiments for periodization in two dimensions. We present numerical evidence for central limit behavior similar to the one-dimensional case and summarize our results in the form of a conjecture. Such central limit behavior has been observed in numerical experiments reported in [34] in the context of heterogeneous multiscale methods.

Central limit results for the convergence of solution u^ϵ to the homogenized limit u^0 may be found in [3, 6]. In contrast, our central limit results are concerned with the convergence of the diffusion tensor $\mathcal{A}^\rho$ to the homogenized tensor $\mathcal{A}^0$.

To solve the periodic homogenization problem for each ρ, we apply periodic boundary conditions to the unit cell in the traditional way as in [4]. In the context of periodization, other types of boundary conditions have also been considered for the unit cell problem. E.g., it is shown in [7] that (21) holds with null Dirichlet or Neumann boundary conditions. Numerical experiments in [34] in the context of heterogeneous multiscale methods indicate, however, that in practice the choice of periodic boundary conditions yields faster convergence in periodization.

7.1 Periodization in One-dimensional Media

For $\omega \in \Omega$ consider the one-dimensional version of the boundary value problem (4):

$$\begin{cases} -\big(a_T(x,\omega)u'(x,\omega)\big)' = f(x) \quad \text{in } \mathcal{D} = (0,1), \\ u(0,\omega) = u(1,\omega) = 0, \end{cases} \tag{22}$$

where $a_T(x,\omega) = a\big(T_x(\omega)\big)$ and a is the one-dimensional counterpart of $\mathcal{A}$ in Section 2.5. Specializing Theorem 2 to one dimension, it can be shown that for almost all $\omega \in \Omega$ the problem (22) admits homogenization with the homogenized coefficient given by

$$\bar{a} = \frac{1}{E\left\{\frac{1}{a}\right\}}. \tag{23}$$

To approximate $\bar{a}$ numerically we can use the method of periodization as follows. Denote $S_\rho = (0,\rho)$ and let

$$a^\rho_{\rm per}(x,\omega) = a_T(x \bmod S_\rho, \omega) = a\big(T_{x \bmod S_\rho}(\omega)\big), \quad x \in \mathbf{R}, \omega \in \Omega. \tag{24}$$

For each $\rho > 0$, $\epsilon > 0$, and $\omega \in \Omega$, we consider the periodized problem,

$$\begin{cases} -\big(a^\rho_{\rm per}(\frac{x}{\epsilon},\omega)u_\rho'(x,\omega)\big)' = f(x) \quad \text{in } \mathcal{D} = (0,1), \\ u_\rho(0,\omega) = u_\rho(1,\omega) = 0. \end{cases} \tag{25}$$

The effective conductivity of this medium as $\epsilon \to 0$ can be computed using the standard homogenization theory; cf. [4]:

$$\bar{a}^\rho(\omega) = \frac{1}{\frac{1}{\rho}\int_0^\rho \frac{1}{a^\rho_{\rm per}(x,\omega)}\mathrm{d}x}. \tag{26}$$

The general convergence result in (21) states that $\bar{a}^\rho(\omega) \to \bar{a}$ almost surely as $\rho \to \infty$. However, due to the special nature of the problem in 1D we may produce a simple proof with an explicit limit.

Theorem 4 For almost all $\omega \in \Omega$, $\bar{a}^\rho(\omega) \to \bar{a}$, as $\rho \to \infty$ with $\bar{a}$ as in (23).

Proof First note that using the change of variable $x \to x/\rho$ in (26) we get

$$\bar{a}^\rho(\omega) = \frac{1}{\int_0^1 \frac{1}{a^\rho_{\rm per}(\rho x,\omega)}\mathrm{d}x} = \frac{1}{\int_0^1 \frac{1}{a_T(\rho x,\omega)}\mathrm{d}x}, \tag{27}$$

where the second equality follows from the fact that for $x \in S_1$,

$$a^{\rho}_{\rm per}(\rho x, \omega) = a_T(\rho x \bmod S_{\rho}, \omega) = a_T(\rho x, \omega). \tag{28}$$

By Birkhoff's Ergodic Theorem we conclude that for almost all $\omega \in \Omega$, as $\rho \to \infty$,

$$\frac{1}{a_T(\rho x, \omega)} \rightharpoonup E\left\{\frac{1}{a}\right\} \quad \text{ in } L^2(\mathcal{D}), \tag{29}$$

therefore,

$$\int_0^1 \frac{1}{a_T(\rho x, \omega)} \mathrm{d}x \to E\left\{\frac{1}{a}\right\}, \quad \text{ as } \rho \to \infty. \tag{30}$$

But then it follows from (27) that for almost all $\omega \in \Omega$,

$$\lim_{\rho \to \infty} \bar{a}^{\rho}(\omega) = \lim_{\rho \to \infty} \frac{1}{\int_0^1 \frac{1}{a_T(\rho x, \omega)} \mathrm{d}x} = \frac{1}{E\left\{\frac{1}{a}\right\}}. \qquad \square$$

7.2 Periodization of Tile-based Media

From this point on, we consider periodization in the context of tile-based random media which we constructed in Section 4. Recall that in the case of tile-based media, a sample point $\omega \in \Omega$ is a pair (s, τ) where $s \in S$ fixes a random structure and $\tau \in \mathbf{Tor}^n$ is a shift. We note that shifting a structure does not change its homogenization property; that is $\mathcal{A}(s, \tau)$ admits homogenization $\mathcal{A}^0$ if and only if $\mathcal{A}(s, 0)$ admits homogenization $\mathcal{A}^0$. One may also verify $\lim\limits_{\rho \to \infty} \mathcal{A}^{\rho}(s, \tau) = \mathcal{A}^0$ if and only if $\lim\limits_{\rho \to \infty} \mathcal{A}^{\rho}(s, 0) = \mathcal{A}^0$. Therefore, when discussing numerical simulations and periodization it suffices to consider only unshifted media. This essentially amounts to sampling elements from a set of full measure in S.

7.2.1 A Central Limit Theorem for One-dimensional Tile-based Media

We begin this section by considering the one-dimensional version of the tile based random media introduced in Section 4. Thus the medium consists of an infinite sequence of segments of unit length whose conductivity profiles is parametrized by the probability space $(Y, \mathcal{F}_Y, \mu_Y)$. Each $y \in Y$ corresponds to a conductivity profile, f_y, which is a function (not necessarily constant) from $\mathbf{Tor}^1$ to $\mathbf{R}$. The ellipticity condition is:

$$0 < \nu_1 \le f_y(x) \le \nu_2, \quad \text{for all } x \in \mathbf{Tor}^1, \quad \text{for all } \ y \in Y.$$

In the case of 1D tile-based media, the effective conductivity, given in (23), is

$$\frac{1}{\bar{a}} = \int_Y \int_0^1 \frac{1}{f_y(\tau)} \mathrm{d}\tau \mathrm{d}\mu_Y(y). \tag{31}$$

We shall establish the rate of convergence of $\bar{a}^{\rho}(\omega)$ to $\bar{a}$. Since shifts are immaterial, we let $\bar{a}^{\rho}_0(s) = \bar{a}^{\rho}(s, 0)$ for $s \in S$. We define the random variable $b : Y \to R$ by

$$b(y) = \int_0^1 \frac{1}{f_y(\tau)}\, \mathrm{d}\tau, \quad y \in Y. \tag{32}$$

Let us recall a few basics from asymptotic theory in probability. Given a sequence of random variables, $\{X_n\}$, we write $X_n \xrightarrow{D} X$ to denote convergence in distribution [32].

Definition 5 [8, page 209] A sequence $\{X_n\}$ of random variables is said to be asymptotically normal with mean m_n and standard deviation σ_n if $\sigma_n > 0$ for n sufficiently large and $\frac{X_n - m_n}{\sigma_n} \xrightarrow{D} Z$, as $n \to \infty$, with $Z \sim N(0,1)$. In this case we use the notation, X_n is $AN(m_n, \sigma_n^2)$ as $n \to \infty$.

The following result will be useful in what follows:

Lemma 2 [8, page 210] If X_n is $AN(m, \sigma_n^2)$, where $\sigma_n \to 0$ as $n \to \infty$, and if g is a function differentiable at m with $g'(m) \neq 0$, then $g(X_n)$ is $AN\big(g(m), (g'(m))^2\sigma_n^2\big)$.

The main result of this section is:

Theorem 5 The sequence $\{\bar{a}_0^\rho\}_{\rho\in\mathbf{N}}$ is $AN\big(\frac{1}{m}, \frac{\sigma^2}{m^4\rho}\big)$ as $\rho \to \infty$, with $m = E\{b\}$ and $\sigma^2 = \mathrm{Var}\{b\}$ where b is as in (32).

Proof For $\omega = (s, 0) = \big(\{s_j\}, 0\big) \in \Omega$, let

$$b_i(s) = \int_0^1 \frac{1}{f_{s_i}(x)}\mathrm{d}x,$$

and note that

$$\int_0^\rho \frac{1}{a_{\mathrm{per}}^\rho(x,\omega)}\mathrm{d}x = \sum_{i=1}^\rho b_i(s),$$

and for each i, $E\{b_i\} = E\{b\} = m$ and $\mathrm{Var}\{b_i\} = \mathrm{Var}\{b\} = \sigma^2$. Let $X_\rho = \frac{1}{\rho}\sum\limits_{i=1}^{\rho} b_i$. Since b_i are i.i.d. with mean m and variance σ^2, we have, by the Central Limit Theorem, that as $\rho \to \infty$, X_ρ is $AN\big(m, \frac{\sigma^2}{\rho}\big)$. Applying Lemma 2 with $g(X) = 1/X$, we obtain,

$$g(X_\rho) \text{ is } AN\Big(g(m), \frac{\big(g'(m)\big)^2\sigma^2}{\rho}\Big).$$

Since $\bar{a}_0^\rho = g(X_\rho) = 1/X_\rho$, then as $\rho \to \infty$,

$$\bar{a}_0^\rho \text{ is } AN\Big(\frac{1}{m}, \frac{\sigma^2}{m^4\rho}\Big). \qquad \square$$

Remark 5 The above result suggests that for large ρ, the sequence of periodized approximations $\bar{a}_0^\rho$ behave as

$$\bar{a}_0^\rho \sim \frac{1}{m} + \frac{1}{\sqrt{\rho}} N\Big(0, \frac{\sigma^2}{m^4}\Big),$$

which gives a rate of convergence of $\rho^{-1/2}$ for periodization in 1D.

7.2.2 Numerical Experiments in 1D

In this section we present the results of simulations of one-dimensional tile-based random media which serve two purposes: (a) to illustrate the results of the previous sections and (b) to motivate the more involved two-dimensional setting in the subsequent sections.

We consider a random structure where the conductivity profile for each tile $y \in Y$ is the constant function given by $f_y(\tau) = y$ for all $\tau \in \mathbf{Tor}^1$, with $Y = [1, 2]$ equipped with the Lebesgue measure; that is, the conductivity of each tile is a uniform random variable in $[1, 2]$. Figure 7 depicts the conductivity function for a particular realization of such a medium. The effective conductivity $\bar{a}$ may be computed explicitly using (31):

$$\bar{a} = \Big(\int_1^2 \int_0^1 \frac{1}{y}\mathrm{d}\tau\mathrm{d}y\Big)^{-1} = \frac{1}{\ln 2}.$$

The random variable b defined in (32), becomes $b(y) = 1/y$, and thus, we have $E\{b\} = \ln 2$ and $\mathrm{Var}\{b\} = E\{b^2\} - \left(E\{b\}\right)^2 = 1/2 - (\ln 2)^2$.

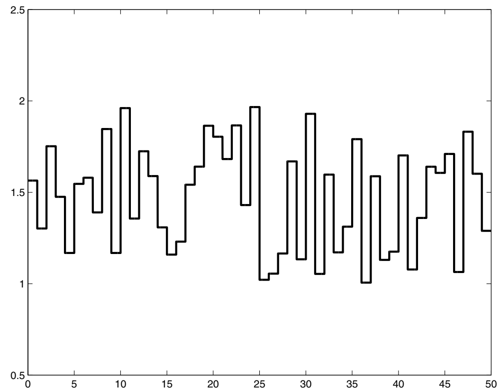

Fig.7 A representative conductivity function of a realization of a random 1D tile-based medium with homogeneous segments

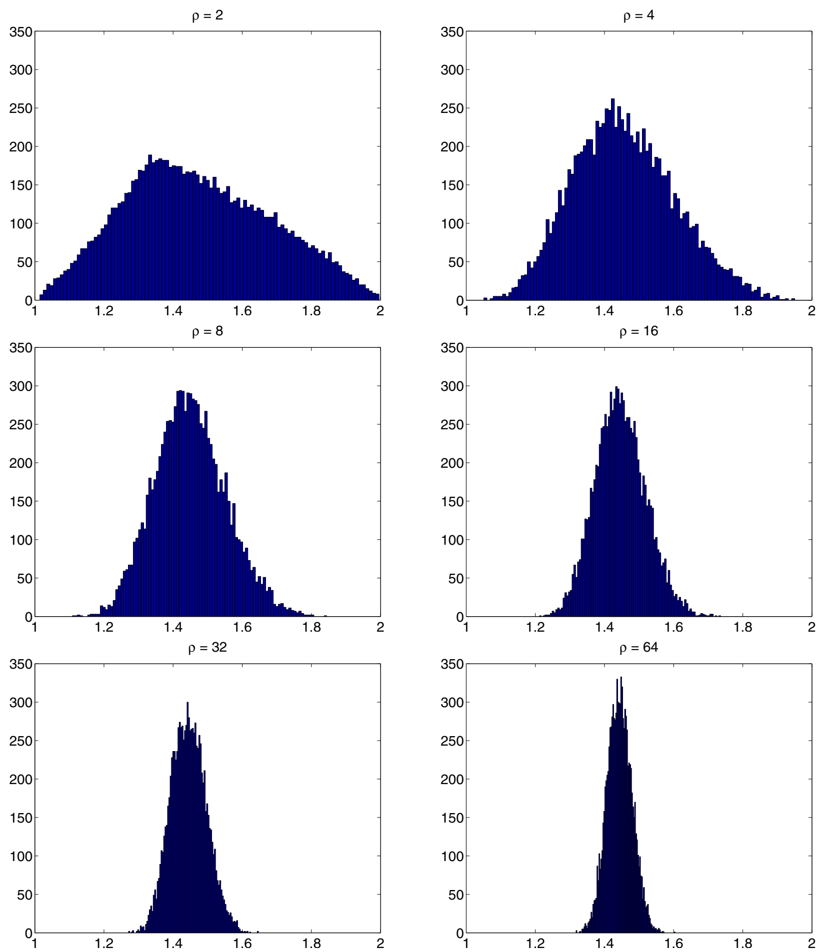

Fig.8 Random 1D tile-based medium with homogeneous segments: distribution of $\bar{a}^\rho$ for different ρ

We compute $\bar{a}^\rho(\omega_j)$ for $\rho = 2^i$, $i = 1, \cdots, 6$ and for realizations ω_j, $j = 1, \cdots, 10000$. The histograms in Figure 8 show the convergence of the approximation $\bar{a}^\rho$ to $\bar{a}$ as ρ gets larger. We note that the distribution of $\bar{a}^\rho$ gets more and more centered around the value of $m = 1/\ln 2 \approx 1.4427$, as expected.

The computational results in Table 1 illustrate the asymptotic behavior of $\bar{a}^\rho$. The columns labeled "Variance", "$\frac{\sigma^2}{m^4\rho}$", and "Ratio", list the sample variance, the asymptotic variance, and their ratio, respectively. We see that the ratio approaches 1, as predicted by Theorem 5. Also, we can see in the log-log plot in Figure 9 the expected asymptotic behavior of $\bar{a}^\rho$ as $\rho \to \infty$.

Table 1 Random 1D tile-based medium with homogeneous segments: Asymptotic behavior of $\bar{a}^\rho$ as $\rho \to \infty$. The last column shows the ratio of the sample variance and the asymptotic variance predicted by Theorem 5.

ρ	Mean	Variance	$\frac{\sigma^2}{m^4\rho}$	Ratio
2	1.472096	4.367275e-02	4.233972e-02	1.031484
4	1.457368	2.166391e-02	2.116986e-02	1.023337
8	1.450063	1.070949e-02	1.058493e-02	1.011768
16	1.446389	5.362583e-03	5.292465e-03	1.013249
32	1.444506	2.663250e-03	2.646232e-03	1.006431
64	1.443598	1.325444e-03	1.323116e-03	1.001760

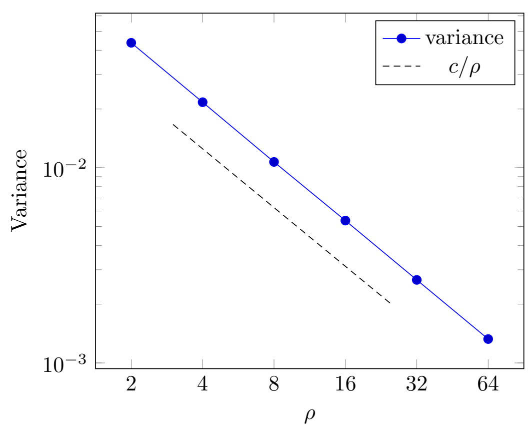

Fig.9 Random 1D tile-based medium with homogeneous segments: Log-log plot of the sample variances for $\bar{a}^\rho$. Also shown is the graph of the theoretical convergence rate of $O(1/\rho)$ for comparison

7.3 Periodization in 2D

We present the results of two sets of computational experiments for estimating the effective properties of checkerboard-like random media. The setup is similar to that presented in Section 5.1, that is, the medium is constructed of two different tiles, say "gray" and "white", which occur with probabilities p and $1 - p$ and have isotropic conductivities:

$$A^{(\text{gray})} = f_1(x)I \quad \text{and} \quad A^{(\text{white})} = f_2(x)I,$$

with

$$f_1(x) = \mathrm{e}^{k \sin \pi x_1 \sin \pi x_2} \quad \text{and} \quad f_2(x) = \mathrm{e}^{-k \sin \pi x_1 \sin \pi x_2}, \tag{33}$$

where $k = 0.3$ and $x = (x_1, x_2) \in \mathbf{Tor}^2$. The computations are more complicated than 1D case because periodization now requires solving a partial differential equation (the unit cell problem) on $\mathbf{Tor}^2$ for each realization. This places limitations, most significantly on computer memory, on how large the cell of periodicity can be. For practical purposes, we choose the largest possible ρ consistent with the available memory, then generate a large number of realizations and compute the periodized coefficients $\mathcal{A}^\rho$ and monitor the sample means and variances. If the standard deviation is sufficiently small, then the sample mean is a good estimator of the desired homogenized coefficient $\mathcal{A}^0$.

These numerical experiments clearly show that effective conductivity matrix, $\mathcal{A}^\rho(\omega)$ is asymptotically normal, however unlike the 1D case, we have no proof at this time. We offer this as a:

Conjecture 1 For 2D tile-based media we have: $\mathcal{A}^\rho_{ij}$ is $AN\big(\mathcal{A}^0, \frac{\sigma_{ij}}{\rho^2}\big)$, as $\rho \to \infty$, for $i, j = 1, 2$, where σ_{ij} does not depend on ρ.

In [7] it is shown that the rate of convergence of of periodization in general random media is of the form $O(\rho^{-\beta})$. The exponent β depends on the mixing properties of the medium and is difficult to estimate in general. According to our conjecture, $\beta = 2$ for 2D tile-based media.

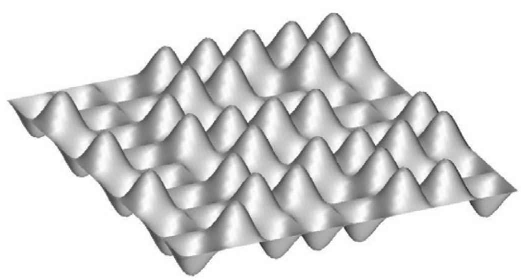

Fig.10 The graph of the conductivity function of a realization of the random checkerboard, according to equation (33)

7.3.1 Numerical Experiment #1 in 2D

Here we consider the case of $p = 1/2$. This is rather special because $\mathcal{A}^0$ can be determined explicitly. The following result which we state as a theorem, is shown on page 234 of [19]:

Theorem 6 Let Q be the 2×2 matrix of rotation by 90 degrees. Suppose $\mathcal{A}$ be Q-invariant. Additionally, assume that there exists a mapping $\phi \in \mathrm{Aut}(\Omega)$ such that $\mathcal{A}\big(\phi(\omega)\big)\mathcal{A}(\omega) = kI$ for a.a. $\omega \in \Omega$, and $\phi^{-1}\big(T_x(\omega)\big) = T_x\big(\phi^{-1}(\omega)\big)$. Then $\mathcal{A}^0 = \sqrt{k}I$.

Let us verify that our random checkerboard satisfies the assumptions of the theorem. First, note that the conductivity $\mathcal{A}$ is Q-invariant because the functions f_1 and f_2 in (33) are invariant under 90 degree rotations. Second, the mapping ϕ in the statement of the theorem may be chosen as follows. For any $\omega = (s, \tau) \in \Omega$ define $\tilde{\omega} = (\tilde{s}, \tau)$ where

$$\tilde{s}_j = \begin{cases} \text{white} & \text{if } s_j = \text{gray}, \\ \text{gray} & \text{if } s_j = \text{white}. \end{cases}$$

Then let $\phi(\omega) = \tilde{\omega}$. It is easy to see (due to $p = 1/2$) that $\phi \in \mathrm{Aut}(\Omega)$. Third, from the expression (20) for $\mathcal{A}(\omega)$ it follows that: $\mathcal{A}(\phi\omega)\mathcal{A}(\omega) = f_1(\tau)f_2(\tau)I = I$, with f_1 and f_2 defined in (33). Therefore by Theorem 6, the homogenized conductivity is $\mathcal{A}^0 = I$.

Table 2 lists the outcome of our computations with $\rho = 2^i$, $i = 1, \cdots, 6$ averaged over 1000 realizations. We see that the mean of $\mathcal{A}^\rho \to I$ as $\rho \to \infty$, as expected, and the variance is $O(\rho^{-2})$ consistent with the conjecture made above. See also the log-log plot in Figure 11 which shows that the variance for $[\mathcal{A}^\rho]_{11}$ is $O(\rho^{-2})$. The histograms in Figure 12 show the evolution of the distribution of $[\mathcal{A}^\rho]_{11}$ toward normal as ρ increases. To further bring this to light, we provide a close-up of the histogram for the $\rho = 64$ case in Figure 13.

Table 2 Experiment 1 of the random checkerboard: Asymptotic behavior of components of $\mathcal{A}^\rho$ as $\rho \to \infty$. The column labeled 'Ratio' shows the ratio of two consecutive variances. The variance shrinks by a factor of four with each doubling of ρ.

$[\mathcal{A}^\rho]_{11}$

ρ	Mean	Variance	Ratio
2	0.99939138	3.87392708e-03	—
4	0.99900417	8.29923510e-04	4.6678
8	0.99972096	2.15407332e-04	3.8528
16	0.99974253	5.64378707e-05	3.8167
32	1.00003515	1.46838211e-05	3.8435
64	0.99997816	3.62430817e-06	4.0515

$[\mathcal{A}^\rho]_{22}$

ρ	Mean	Variance	Ratio
2	0.99960898	3.87415798e-03	—
4	0.99886380	8.18404811e-04	4.7338
8	0.99971593	2.15090563e-04	3.8049
16	0.99973093	5.63314550e-05	3.8183
32	1.00003600	1.45179876e-05	3.8801
64	0.99997095	3.58908744e-06	4.0450

$[\mathcal{A}^\rho]_{12}$

ρ	Mean	Variance	Ratio
2	0.00000000	0.00000000e+00	—
4	-0.00001521	5.17427142e-07	0.0000
8	-0.00001938	2.21103369e-07	2.3402
16	-0.00000147	6.44481557e-08	3.4307
32	-0.00000278	1.63013662e-08	3.9535
64	-0.00000056	4.11889874e-09	3.9577

$[\mathcal{A}^\rho]_{21}$

ρ	Mean	Variance	Ratio
2	0.00000000	0.00000000e+00	—
4	-0.00001521	5.17427142e-07	0.0000
8	-0.00001938	2.21103369e-07	2.3402
16	-0.00000147	6.44481557e-08	3.4307
32	-0.00000278	1.63013662e-08	3.9535
64	-0.00000056	4.11889874e-09	3.9577

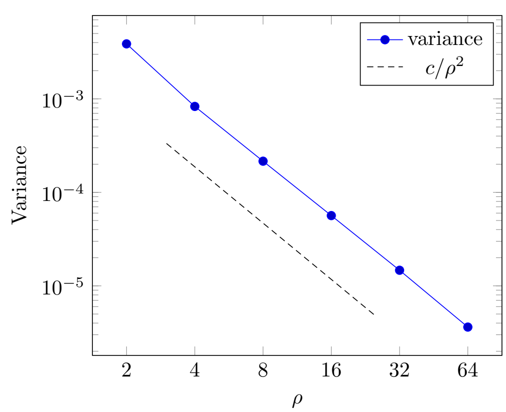

Fig.11 Experiment 1 of the random checkerboard: Log-log plot of the sample variances for $[\mathcal{A}^\rho]_{11}$. Also shown is the graph of the conjectured convergence rate of $O(1/\rho^2)$ for comparison

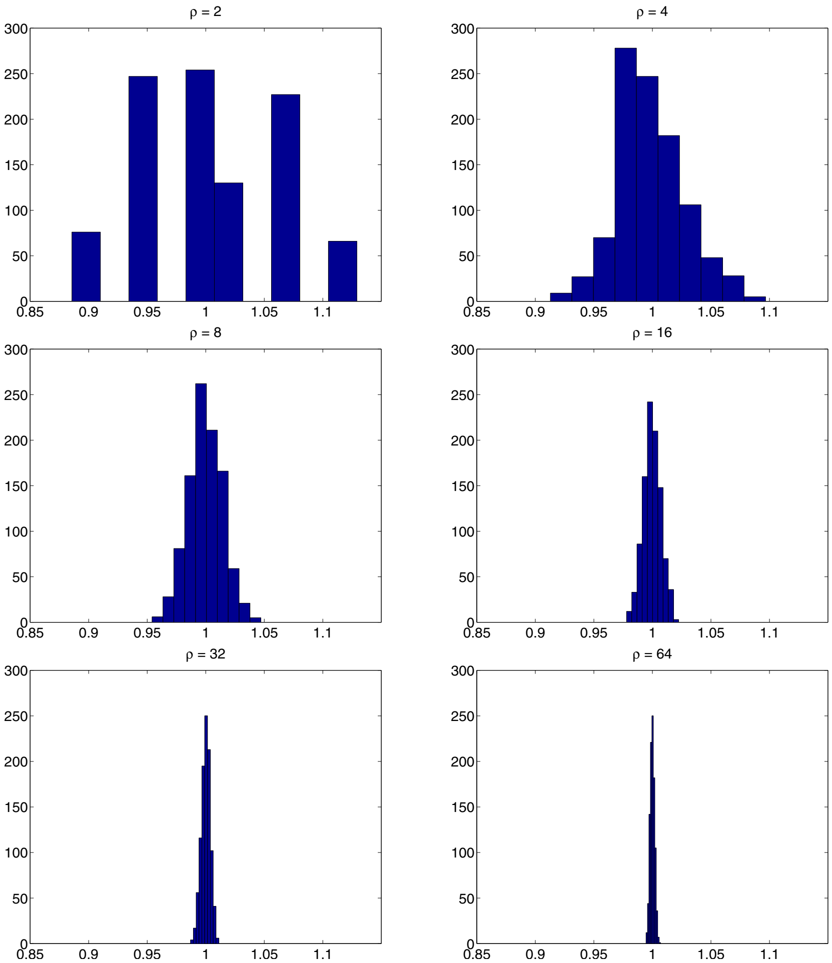

Fig.12 Experiment 1 of the random checkerboard: Distributions of $[\mathcal{A}^{\rho}]_{11}$ for $\rho = 2, 4, 8, 16, 32, 64$, generated with 1000 realizations

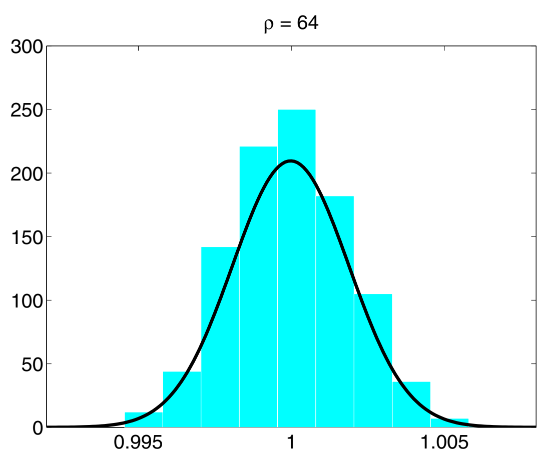

Fig.13 Experiment 1 of the random checkerboard: A close-up of the histogram (1000 samples) for the distribution of $[\mathcal{A}^{\rho}]_{11}$ with $\rho = 64$. Superimposed is the graph of the normal distribution with mean and variance equal to the sample mean and variance

7.3.2 Numerical Experiment #2 in 2D

This set of experiments are identical with those in the previous section except we let $p = 1/4$. The effective conductivity, $\mathcal{A}^0$, will be isotropic by Remark 4, however there is no longer an explicit formula for its value.

Table 3 lists the outcome of our computations with $\rho = 2^i$, $i = 1, \cdots, 6$ averaged over 1000 realizations. We see that the mean of $\mathcal{A}^\rho$ approaches a multiple of identity as $\rho \to \infty$, as expected, and the variance is $O(\rho^{-2})$ consistent with the conjecture made above. See also the log-log plot in Figure 14 which shows that the variance for $[\mathcal{A}^\rho]_{11}$ is $O(\rho^{-2})$. The histograms in Figure 15 show the evolution of the distribution of $[\mathcal{A}^\rho]_{11}$ toward normal as ρ increases. To further bring this to light, we provide a close-up of the histogram for the $\rho = 64$ case in Figure 16.

Table 3 Experiment 2 of the random checkerboard: Asymptotic behavior of components of $\mathcal{A}^\rho$ as $\rho \to \infty$. The column labeled 'Ratio' shows the ratio of two consecutive variances. The variance shrinks by a factor of four with each doubling of ρ.

$[\mathcal{A}^\rho]_{11}$

ρ	Mean	Variance	Ratio
2	0.94149083	2.45200172e-03	—
4	0.94089838	5.87271432e-04	4.1752
8	0.94140841	1.49404258e-04	3.9308
16	0.94096033	3.83403355e-05	3.8968
32	0.94107328	9.47318479e-06	4.0472
64	0.94100935	2.55592740e-06	3.7064

$[\mathcal{A}^\rho]_{22}$

ρ	Mean	Variance	Ratio
2	0.94158409	2.46292264e-03	—
4	0.94093164	5.88741898e-04	4.1834
8	0.94137233	1.48839971e-04	3.9555
16	0.94095308	3.82877003e-05	3.8874
32	0.94108655	9.39411259e-06	4.0757
64	0.94101763	2.54854442e-06	3.6861

$[\mathcal{A}^\rho]_{12}$

ρ	Mean	Variance	Ratio
2	0.00000000	0.00000000e+00	—
4	-0.00001179	2.80617913e-07	0.0000
8	-0.00000886	1.21840925e-07	2.3031
16	0.00000576	2.98058477e-08	4.0878
32	0.00000179	7.23335555e-09	4.1206
64	0.00000003	1.90536287e-09	3.7963

$[\mathcal{A}^\rho]_{21}$

ρ	Mean	Variance	Ratio
2	0.00000000	0.00000000e+00	—
4	-0.00001179	2.80617913e-07	0.0000
8	-0.00000886	1.21840925e-07	2.3031
16	0.00000576	2.98058477e-08	4.0878
32	0.00000179	7.23335555e-09	4.1206
64	0.00000003	1.90536287e-09	3.7963

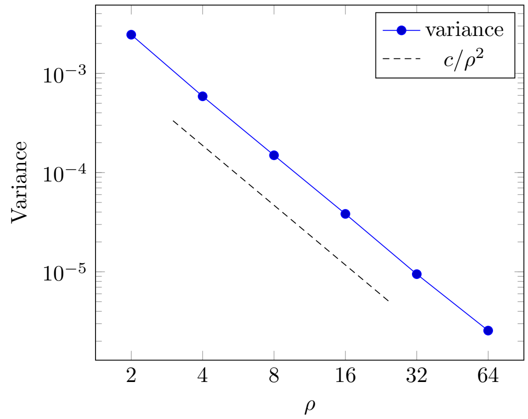

Fig.14 Experiment 2 of the random checkerboard: Log-log plot of the sample variances for $[\mathcal{A}^\rho]_{11}$. We see the constant slope which indicates the observed rate of convergence. Also shown is the graph of the conjectured convergence rate of $O(1/\rho^2)$ for comparison

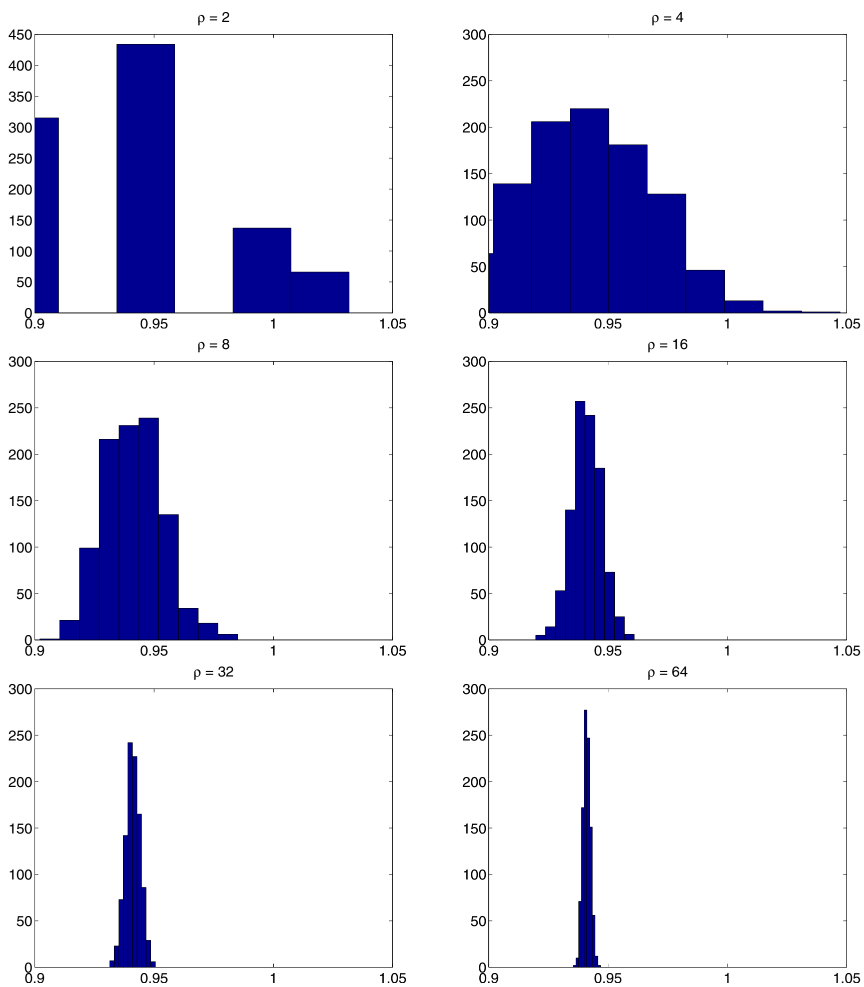

Fig.15 Experiment 2 of the random checkerboard: Distributions of $[\mathcal{A}^\rho]_{11}$ for $\rho = 2, 4, 8, 16, 32, 64$, generated with 1000 realizations

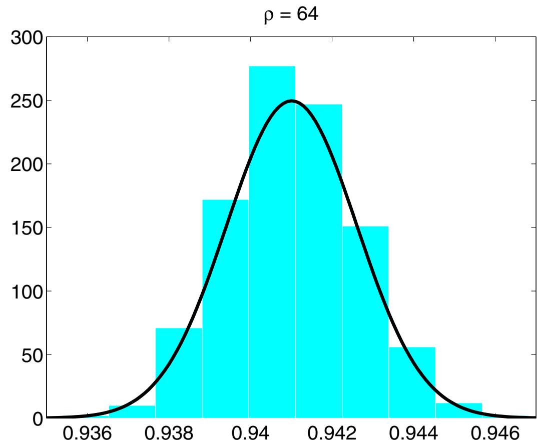

Fig.16 Experiment 2 of the random checkerboard: A close-up of the histogram for Distributions of $[\mathcal{A}^\rho]_{11}$ with $\rho = 64$

References

[1] Alexanderian A, Rathinam M, Rostamian R. Irreducibility of a symmetry group implies isotropy. J Elasticity, 2011, **102**(2): 151–174

[2] Alicandro R, Cicalese M, Gloria A. Integral representation results for energies defined on stochastic lattices and application to nonlinear elasticity. Arch Ration Mech Anal, 2011, **200**(3): 881–943

[3] Bal G. Central limits and homogenization in random media. Multiscale Modeling & Simulation, 2008, **7**(2): 677–702

[4] Bensoussan A, Lions J L, Papanicolaou G. Asymptotic Analysis for Periodic Structures. Volume 5 of Studies in Mathematics and its Applications. Amsterdam: North-Holland Publishing Co, 1978

[5] Berdichevsky V, Jikov V, Papanicolaou G. Homogenization. Volume 50 of Series on Advances in Mathematics for Applied Sciences. River Edge, NJ: World Scientific Publishing Co Inc, 1999

[6] Bourgeat A, Piatnitski A. Estimates in probability of the residual between the random and the homogenized solutions of one-dimensional second-order operator. Asym Anal, 1999, **21**(3/4): 303–315

[7] Bourgeat A, Piatnitski A. Approximations of effective coefficients in stochastic homogenization. Ann Inst H Poincaré Probab Statist, 2004, **40**(2): 153–165

[8] Brockwell P J, Davis R A. Time Series: Theory and Methods. Springer Series in Statistics. 2nd ed. New York: Springer-Verlag, 1991

[9] Byström J, Dasht J, Wall P. A numerical study of the convergence in stochastic homogenization. J Anal Appl, 2004, **2**(3): 159–171

[10] Byström J, Engström J, Wall P. Periodic approximation of elastic properties of random media. Adv Algebra Anal, 2006, **1**(2): 103–113

[11] Chechkin G A, Piatnitski A L, Shamaev A S. Homogenization. Volume 234 of Translations of Mathematical Monographs. Methods and Applications, Translated from the 2007 Russian Original by Tamara Rozhkovskaya. Providence, RI: American Mathematical Society, 2007

[12] Cioranescu D, Donato P. An Introduction to Homogenization. Volume 17 of Oxford Lecture Series in Mathematics and its Applications. New York: The Clarendon Press Oxford University Press, 1999

[13] Cornfeld I P, Fomin S V, Sinaǐ Ergodic Theory. Volume 245 of Grundlehren der Mathematischen Wissenschaften [Fundamental Principles of Mathematical Sciences]. New York: Springer-Verlag, 1982

[14] Efendiev Y, Pankov A. Numerical homogenization and correctors for nonlinear elliptic equations. SIAM J Appl Math, 2004, **65**(1): 43–68 (electronic)

[15] Efendiev Y, Pankov A. Numerical homogenization of nonlinear random parabolic operators. Multiscale Model Simul, 2004, **2**(2): 237–268 (electronic)

[16] Fulton W, Harris J. Representation Theory. Volume 129 of Graduate Texts in Mathematics. New York: Springer-Verlag, 1991

[17] Gloria A, Otto F. An optimal variance estimate in stochastic homogenization of discrete elliptic equations. Ann Probab, 2011, **39**(3): 779–856

[18] James G, Liebeck M. Representations and Characters of Groups. 2nd ed. New York: Cambridge University Press, 2001

[19] Jikov V V, Kozlov S M, Oleĭnik O A. Homogenization of Differential Operators and Integral Functionals. Berlin: Springer-Verlag, 1994

[20] Kozlov S M. The averaging of random operators. Mat Sb (NS), 1979, **109**(151)(2): 188–202, 327

[21] Oleĭnik O A, Shamaev A S, Yosifian G A. Mathematical Problems in Elasticity and Homogenization. Volume 26 of Studies in Mathematics and its Applications. Amsterdam: North-Holland Publishing Co, 1992

[22] Owhadi H. Approximation of the effective conductivity of ergodic media by periodization. Probab Theory Related Fields, 2003, **125**(2): 225–258

[23] Pankov A. G-convergence and Homogenization of Nonlinear Partial Differential Operators. Volume 422 of Mathematics and its Applications. Dordrecht: Kluwer Academic Publishers, 1997

[24] Papanicolaou G C, Varadhan S R S. Boundary value problems with rapidly oscillating random coefficients//Random Fields, Vol I, II (Esztergom, 1979). Volume 27 of Colloq Math Soc János Bolyai. Amsterdam: North-Holland, 1981: 835–873

[25] George C. Papanicolaou. Diffusion in random media//Keller J B, McLaughlin D, Papanicolaou G C. Surveys in Applied Mathematics, Vol 1. New York: Plenum, 1995: 205–253

[26] Sab K. On the homogenization and the simulation of randommaterials. European J Mech A Solids, 1992, **11**(5): 585–607

[27] Sánchez-Palencia E. Nonhomogeneous Media and Vibration Theory. Volume 127 of Lecture Notes in Physics. Berlin: Springer-Verlag, 1980

[28] Schur I. Neue begründung der theorie der gruppencharaktere. Sitzungsberichte der Königlich Preuβischen Akademie der Wissenschaften zu Berlin, Part 1, 1905: 406–432

[29] Telega J J, Bielski W. Stochastic homogenization and macroscopic modelling of composites and flow through porous media. Theoret Appl Mech, 2002, **28/29**: 337–377

[30] Walters P. An Introduction to Ergodic Theory. Volume 79 of Graduate Texts in Mathematics. New York: Springer-Verlag, 1982

[31] Weyl H. The Classical Groups. Princeton Landmarks in Mathematics. 2nd ed. Princeton, NJ: Princeton University Press, 1946

[32] Williams D. Probability with Martingales. Cambridge Mathematical Textbooks. Cambridge: Cambridge University Press, 1991

[33] Wu X H, Efendiev Y, Hou T Y. Analysis of upscaling absolute permeability. Discrete Contin Dyn Syst Ser B, 2002, **2**(2): 185–204

[34] Yue X, E Weinan. The local microscale problem in the multiscale modeling of strongly heterogeneous media: Effects of boundary conditions and cell size. J Comput Phy, 2007, **222**(2): 556–572

[35] Yurinskiĭ V V. Averaging of symmetric diffusion in a random medium. Akademiya Nauk SSSR, Sibirskoe Otdelenie, Sibirskiĭ Matematicheskiĭ Zhurnal, 1986, **27**(4): 167–180; English translation: Siberian Math J, 1986, **27**(4): 603–613

[36] Zhikov V V, Pyatnitskiĭ A L. Homogenization of randomsingular structures and random measures. Izvestiya Mathematics, 2006, **70**(1): 19–67